Journal of Energy Chemistry 52 (2021) 102–114

Contents lists available at ScienceDirect

Journal of Energy Chemistry

journal homepage: www.elsevier.com/locate/jechem

http://www.journals.elsevier.com/journal-of-energy-chemistry/

Review

Intermediates transformation for efficient perovskite solar cells

Zhizai Li [a,1], Yi Sun [b,1], Huanhuan Yao [a], Jing Zhao [a], Qian Wang [a,*], Liming Ding [c,*], Zhiwen Jin [a,*]

[a] School of Physical Science and Technology & Key Laboratory for Magnetism and Magnetic Materials of MoE & Key Laboratory of Special Function Materials and Structure Design, MoE & National & Local Joint Engineering Laboratory for Optical Conversion Materials and Technology, Lanzhou University, Lanzhou 730000, Gansu, China
[b] School of Physics, Changji University, Changji 830100, Xinjiang Uygur Autonomous Region, China
[c] Center for Excellence in Nanoscience (CAS), Key Laboratory of Nanosystem and Hierarchical Fabrication (CAS), National Center for Nanoscience and Technology, Beijing 100190, China

ARTICLE INFO

Article history:
Received 18 March 2020
Revised 25 April 2020
Accepted 26 April 2020
Available online 05 May 2020

Keywords:
Intermediate
Formation energy
Crystalline dynamics
Solubility
Nucleation sites

ABSTRACT

Perovskite materials have made a great progress in terms of the power conversion efficiency (PCE), rising from 3.8% to 25.2%. To obtain pinhole-free, superior crystal, and high-quality perovskite films with less defect, intermediates transformation is important, which has been clearly studied and widely applied. In this review, we systematically summarize the commonly formed intermediates and detailedly analyze their mechanisms from five aspects: (1) Solvent-induced intermediate; (2) HI-induced intermediate; (3) CH_3NH_2-induced intermediate; (4) MAAc-induced intermediate; (5) other intermediates. Finally, we also provide some prospects on high-quality perovskite fabrication based on using intermediates prudently.

Zhizai Li received his B.S. degree in the School of Physical Science and Technology, Lanzhou University. He is currently a Ph.D. student under the supervision of Prof. Zhiwen Jin. His main research focuses on inorganic semiconductor materials and solar cells.

Huanhuan Yao received her B.S. degree in the School of Physics and Electronic Engineering, Northwest Normal University. She is currently a M.S. student at Lanzhou University. Her main research focuses on organic-inorganic hybrid semiconductor materials and solar cells.

Yi Sun, Associate Professor of Changji University, received the B.S. degree and M.S. degree from Xinjiang University in 2003 and 2006, received Ph. D. degree from Shandong University in 2012, He joined Changji University in 2006. His research interests include Thin-film photoelectric materials, thermoelectric materials, and energy conversion related devices.

Jing Zhao received her B.S. degree in the School of Optoelectronic Engineering, Changzhou Institute of technology. She is currently a M.S. student at Lanzhou University. Her main research focuses on inorganic semiconductor materials and solar cells.

* Corresponding authors.
E-mail addresses: qianwang@lzu.edu.cn (Q. Wang), ding@nanoctr.cn (L. Ding), jinzw@lzu.edu.cn (Z. Jin).
[1] These authors contributed equally to this work.

https://doi.org/10.1016/j.jechem.2020.04.047

Qian Wang is a researcher with the School of Physical Science and Technology, Lanzhou University. She has received her B.S. and Ph.D. degree in Materials Chemistry from Lanzhou University of China in 2011 and 2016, respectively. She joined Lanzhou University in 2018. Most recently her research interest focuses on quantum dots based device and structural design in optoelectronic device.

Liming Ding got Ph.D. degree from University of Science and Technology of China. He started his research on OSCs and PLEDs in Olle Inganäs Lab in 1998. Later on, he worked with Frank Karasz and Tom Russell at PSE, UMASS Amherst. He joined Konarka as a Senior Scientist in 2008. In 2010, he joined National Center for Nanoscience and Technology as a Full Professor. His research interests include perovskite solar cells, organic solar cells and photodetectors.

Zhiwen Jin received the B.S. degree from Lanzhou University in 2011 and Ph.D. degree from Institute of Chemistry, Chinese Academy of Sciences in 2016. He joined Lanzhou University in 2018 as a professor with the School of Physical Science and Technology, Lanzhou University. His research interests include inorganic semiconductor materials, thin-film photoelectric devices and device physics.

1. Introduction

Nowadays, perovskite solar cells (PSCs) attract lots of attentions, and tremendous breakthroughs have been made, which can be ascribed to the remarkable optoelectronic properties of perovskite materials, such as long carriers diffusion, strong light absorption, low exciton binding energy and outstanding carrier recombination lifetime [1–4]. Hitherto, the state-of-the-art PSCs have shown a certified power conversion efficiency (PCE) with 25.2%, which can compare favourably with silicon solar cells [5–8].

Although the performance of PSCs has great improved, it is still far below the theoretical efficiency of 31.4% [9–11]. One of the primary reasons can be ascribed to poor quality of perovskite films, which trends to induce leakage current and absorption losses [12,13]. Usually, the pin-hole free, large grains, low defects and superior mobility perovskite films can be easily fabricated through solution processes with different solvents [14,15]. Researchers used different solvents, such as dimethyl sulfoxide (DMSO), N,N-Dimethyl formamid (DMF), methylammonium acetate (MAAc) and so on [16–19], to control the crystalline rate and retard the quick reaction in the crystalline process. During the nucleation and growth period, intermediates appeared to control the dense and sequential perovskite film formation [20,21]. Besides, intermediates could increase the nucleation sites to obtain a uniform perovskite film [22]. Apart from these advantages, the intermediates can be adopted to fabricate perovskite in low temperature [23], which shows great prospects in soft substrate. Meanwhile, reduced temperature can induce metastable phase formation in $CsPbX_3$ inorganic perovskite to increase its structural stability [24,25]. However, until now, related reviews lack to systematically summarize advanced works about intermediates.

In this review, we first generally introduce the function of intermediates in the beginning. After that, a significant emphasis will be placed on different kinds of liquid-induced intermediates and detailedly analyzing their physical mechanisms: Polar aprotic solvents induced intermediate and HI-induced intermediate; Meanwhile, MA gas, molten salt, and other materials-induced intermediates are also clearly explored. Finally, we will give a brief summary and outlook about current challenges and opportunities in this field.

2. The significant role of intermediates

Intermediates can be defined as a compound formed between perovskite precursors and small molecules. And the main function of intermediates can be rough summarized as follow:

(1) Changing the crystalline dynastic to retard quick reaction in precursor through ions exchange;
(2) Reducing the activation energy of precursor transform to perovskite films;
(3) Promoting homogeneous nucleation and enable an adjustable perovskite film growth rate;
(4) Inducing lattice strain to influence the phase diagram and transition temperature for avoiding perovskite structure distorting;
(5) Healing the defect for less trap states and forming high-quality perovskite;

The detail information of each intermediate and corresponding devices' performance is listed in Table 1.

3. Solvent forms intermediates

The conventional solvents are DMSO, DMF, N-methyl-2-pyrrolidone (NMP) and γ-butyrolactone (GBL). All of them are polar aprotic solvents (Lewis based) and possess oxygen, sulfur, or nitrogen, making them easily coordinate with Lewis acid (such as PbI_2) [26]. In other words, it can consist with Pb atom and form a dative Pb-O because C-O or S-O bond. Hence, they can adjust crystalline rate and morphology of perovskite [27–30]. Solvents and solution speciation are linked to perovskite quality. Weakly coordinating solvents formed an intermediate and transformed to perovskite after annealing, while strongly coordinating solvents formed perovskite directly [31]. Typically, PbI_2 and other solvents are selected as the intermediates, because ionic bonding in I-Pb-I layer is strong enough, and Van der Waals interaction appears between adjacent sandwiched layers, making PbI_2 possible to be intercalated by different guest molecules [32].

3.1. DMSO-induced intermediate

As early reported, DMSO has sulfoxide oxygen, which made it easily combine with PbI_2 for forming PbI_2(DMSO) intermediate [33–35]. The forming PbI_2(DMSO) intermediate can retard rapid crystal during annealing process and promote perovskite grain growth [36]. Because DMSO intermediate shows a larger polarity value (0.444) than DMF-induce intermediate (0.386), which possible makes its structure more stable [37]. Besides, comparing it with other conventional precursors, DMSO intermediate can lower the activation energy from precursor to perovskite by a two-stage reaction (first stage: precursor to intermediate and second stage: intermediate to perovskite) [38,39].

Table 1
The function of intermediates and corresponding devices' performance.

State	Intermediate	Function	Structure	J_{sc} (mA cm^{-2})	V_{oc} (V)	FF (%)	PCE (%)	Ref.
Liquid	(CH_3NH_3I-PbI_2-DMSO)	Via an intercalation process during the dropwise application of a non-dissolving solvent to retard rapid reaction between MAI and PbI_2.	FTO/TiO_2/MAPb($I_{1-x}Br_x$)$_3$/PTAA/Au	19.65	1.12	76.0	16.72	[40]
	(CH_3NH_3I-PbI_2-DMF)	Increase carrier mobility and crystallinity.	ITO/SnO_2/$MAPbI_{3-x}Cl$/Spiro-OMeTAD/Au	22.03	1.10	78.5	19.20	[49]
	PbI_2(NMP)	Induce a longer carrier life time and longer diffusion coefficient.	FTO/TiO_2/$FAPbI_3$/PTAA/Au	24.50	1.07	74.5	19.50	[54]
	PbI_2(DMSO)	Lower the activation energy from precursor to perovskite and shorter the reaction time.	FTO/TiO_2/$CsPbI_2Br$/Spiro-OMeTAD/Au	14.90	1.18	77.2	13.50	[39]
	PbI_2(DMSO)	Slow the crystallization of the perovskite film.	FTO/TiO_2/$CsPbI_2Br$/Spiro-OMeTAD/Au	15.33	1.22	78.7	14.78	[20]
	PbI_2(DMSO)	Induce molecular exchange between FAI and DMSO at low temperatures during the spinning process.	FTO/TiO_2/$(FAPbI_3)_{1-x}(MAPbBr_3)_x$/PTAA/Au	24.70	1.06	77.5	20.20	[44]
	PbI_2(DMSO)	Suppresses larger grains growth and promote porous PbI_2 formation during anti-solvent extraction.	FTO/TiO_2/$MAPbI_3$/Spiro-OMeTAD/Au	20.46	1.04	74.0	15.66	[45]
	$CuBr_2DMSO_2$	A flowable phase to form larger grains.	ITO/PEDOT:PSS/MAI$(PbI_2)_{1-x}(CuBr_2)_x$/PCBM/LiF/Al	21.51	0.96	82.6	17.09	[42]
	SnI_2·3DMSO	Promote homogeneous nucleation and enable an adjustable perovskite film growth rate.	FTO/TiO_2/$MASnI_3$/Spiro-OMeTAD/Au	15.20	0.67	57.0	5.79	[47]
	DMF-induced intermediate	Induce interaction between solvent molecules and PbI_2 crystal lattice to form uniform thin films.	FTO/TiO_2/$MAPbI_3Cl_{3-x}$/Spiro-OMeTAD/Au	21.40	0.91	71.3	13.80	[48]
	PbX_2-AI-DMSO-DMF	Help to form high-quality perovskite film with low trap states and long-balanced charge-carrier transfer length.	FTO/TiO_2/$FA_xMA_{1-x}PbI_{2.55}Br_{0.45}$/Spiro-OMeTAD/Au	23.72	1.08	78.8	20.11	[28]
	$MAPbI_{3-x}Ac_x$	Retard the quick reaction between MAI and PbI_2 and obtain high quality perovskite films by ionic exchanger between I^- and Ac^-.	ITO/PEDOT:PSS/$MAPbI_3$/PCBM/FPI-PEIE/Ag	22.90	1.00	79.0	18.09	[87]
	$MAPbI_{3-x}Ac_x$	Influence crystalline process by increasing the number of homogeneous nucleation sites for homogeneous nucleation.	FTO/TiO_2/$MAPbI_3$/Spiro-OMeTAD/Au	23.36	1.04	69.2	16.79	[100]
	$MAPbI_3$·xH_2O	Improve the crystalline dynastic and the morphology.	ITO/PEDOT:PSS/$MAPbI_3$/$PC_{61}BM$/C_{60}/BCP/Ag	25.00	1.02	75.0	19.12	[96]
Solid	$HPbI_3$ ($DMAPbI_3$)	Slow down the crystalline process by ionic exchange in the $[PbI_6]^{4-}$ octahedral framework and eliminate the water in the precursor.	FTO/TiO_2/$FAPbI_3$/PTAA/Ag	23.80	0.95	65.0	15.40	[56]
	$HPbI_3$ ($DMAPbI_3$)	Modify the bandgap and increasing the stability of lattice.	FTO/TiO_2/$CsPbI_3$/PTAA/Au	18.95	1.06	74.9	15.07	[66]
	$HPbI_3$ ($DMAPbI_3$)	Induce tensile lattice strain to broaden light absorption range and make perovskite much stable.	FTO/TiO_2/$CsPbI_3$/Carbon	18.50	0.79	65.0	9.50	[67]
	MAI·PbI_2·SC$(NH_2)_2$	Promote grain growth and reduce its roughness.	FTO/TiO_2/$MAPbI_3$/Spiro-MeOTAD/Au	22.49	1.10	75.0	18.46	[92]
	$MAPbI_3$·MACl	Control the delivery speed of PbI_2, the rapid nucleation and near thermodynamic equilibrium subsequent growth were further postponed.	FTO/SnO_2/$MAPbI_3$/Spiro-OMeTAD/Au	21.43	1.06	75.0	17.11	[98]
Gas	$MAPbI_3$·xCH_3NH_2	Induce defect-healing to form high quality films.	FTO/TiO_2/$MAPbI_3$/Spiro-OMeTAD/Ag	19.60	1.08	71.4	15.10	[77]
	$MAPbI_3$·xCH_3NH_2	Decrease impurities at the grain boundaries and separate each grain.	FTO/TiO_2/$MAPbI_3$/Spiro-MeOTAD/Au	20.80	1.08	78.5	17.70	[79]
	$MAPbI_3$·xCH_3NH_2	Increase the infiltration rate of perovskite into TiO_2 and further improve its electron injection to reduce shunting.	ITO/TiO_2/$MAPbI_3$/Spiro-MeOTAD/Au	21.80	1.07	70.7	16.60	[80]
	$MAPbI_3$·xCH_3NH_2	Modify energy level aligning and carrier transporting.	FTO/TiO_2/$MAPbI_3$/Spiro-MeOTAD/Au	19.30	1.06	71.0	14.90	[81]

For one-step method, Seok et al. first used toluene to induce an intermediate appearing, and the intermediate (CH_3NH_3I-PbI_2-DMSO) can retard the rapid reaction of PbI_2 and CH_3NH_3I for preparing high quality MAPb($I_{1-x}Br_x$)$_3$ perovskite film, as shown in Fig. 1(a). They pointed that the CH_3NH_3I-PbI_2-DMSO intermediate influenced the reaction rate between MAI(Br) and PbI(Br) by an intercalation process, which was confirmed by XRD analysis. Because of the controllable reaction rate, the MAPb($I_{1-x}Br_x$)$_3$ PSCs possessed high quality morphology and showed a certified PCE of 16.2% without hysteresis [40]. Park et al. utilized a simple spin-coating method of a DMF solution containing PbI_2, CH_3NH_3I, and DMSO (1:1:1 mol%) to form CH_3NH_3I-PbI_2-DMSO adduct after diethyl ether treatment. The diethyl ether is used to remove DMF and remain DMSO for forming intermediate because the intermediate of DMSO-induced is stable than DMF-induced. Therefore, post annealing yielded high quality perovskite film with a best PCE of 19.7%. Interestingly, they found that this DMSO-induced intermediate showed poor stability because of the gradual vaporization of DMSO from the surface of adduct film, and led to an uneven $MAPbI_3$ film [37]. Then, Han et al. used ethyl acetate (EA) to assist crystallization and remove the residual DMSO in the perovskite film during annealing (noted that toluene can't effectively remove residual DMSO). The reason can be ascribed as EA disrupts the formation of the PbI_2-MAI-DMSO intermediate, therefore DMSO don't coordinate with PbI_2-MAI and thus can be wash away, finally, a high PCE of 15.58% was achieved [41]. Meanwhile, the weak bond of DMSO to CH_3NH_3I-PbI_2 make intermediate (CH_3NH_3-I-PbI_2-DMSO) is not flowable, leading small grains appearing (grains couldn't growth) during the heat-treatment process. Whereafter, Moon et al. used $CuBr_2$·DMSO to partly displace PbI_2·DMSO for forming larger grains with reproducible perovskite film. Different from PbI_2·DMSO complex, $CuBr_2$·$DMSO_2$ powder was melt and further changed into a flowable phase (not simultaneous melt and decomposition). Finally, the PCE was greatly

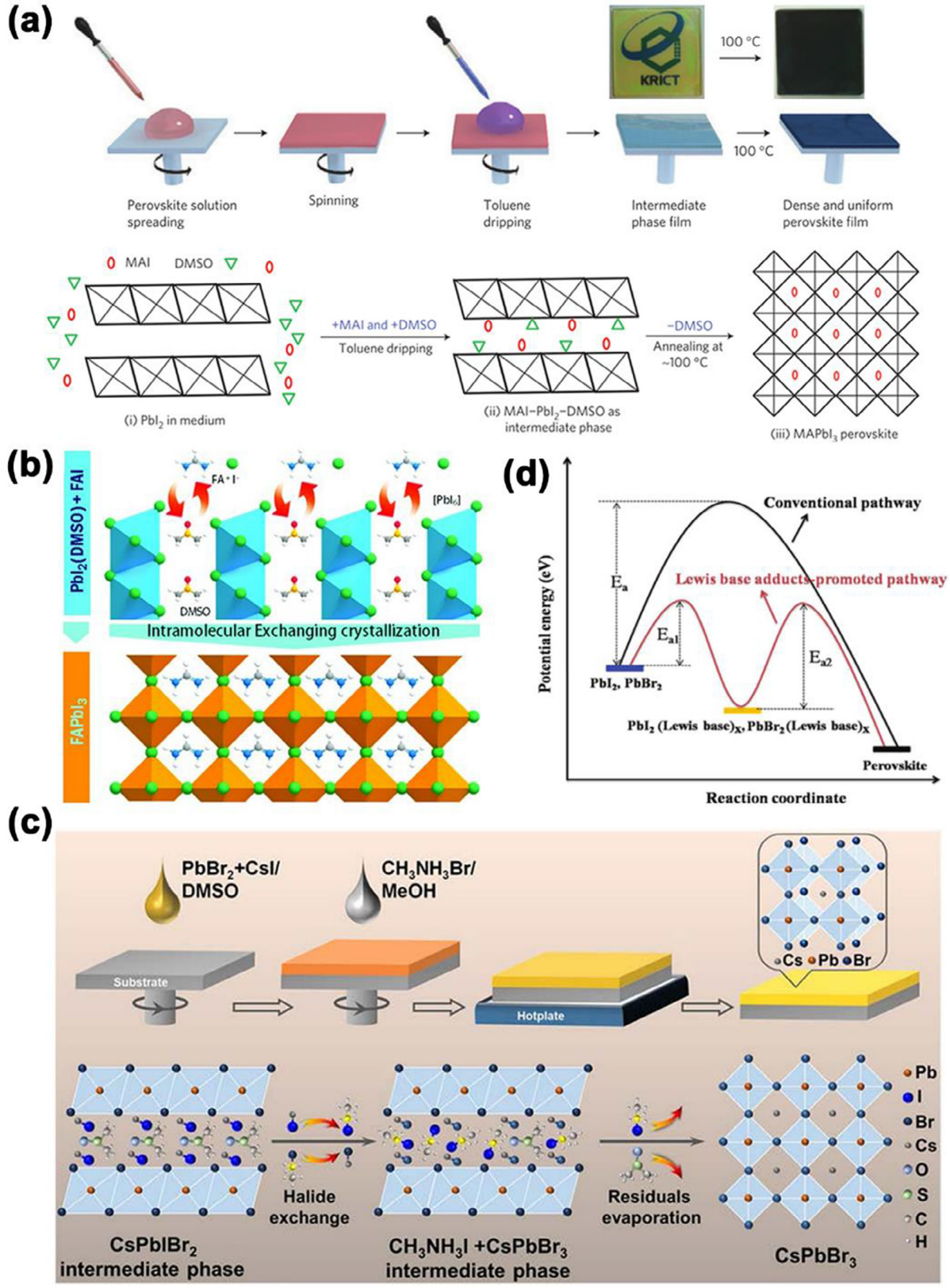

Fig. 1. (a) Preparing the uniform and dense perovskite film via the MAI-PbI_2-DMSO intermediate. Reproduced with permission [40]. Copyright 2014, Nature Publishing Group. (b) Schematics of $FAPbI_3$ crystallization involving the direct intramolecular exchange of DMSO molecules intercalated in PbI_2 with FAI. Reproduced with permission [44]. Copyright 2015, Science Publishing Group. (c) Schematic procedures the formation mechanism of the $CsPbBr_3$ film through intermediate halide exchange. Reproduced with permission [16]. Copyright 2019, American Chemical Society Publications. (d) The reaction coordinate diagram of the inorganic perovskite formation via the conventional pathway and DSMO-adduct promoted pathway. Reproduced with permission [39]. Copyright 2018, Wiley-VCH Publications.

improved from 13.18% to 17.09% without J-V hysteresis [42]. Besides, a perovskite template ($MAPbI_3$-FAI-PbI_2-DMSO) was formed through postdeposition of colloidal CH_3NH_3I-PbI_2-DMSO film with FAI to fabricated high quality α-$FAPbI_3$ film [17]. By inducing a DMSO intermediate called $(MA,FA)_2Pb_3I_8$·2DMSO, Wang et al. decreased the proportion of the small-n 2 dimension (2D) phases and significantly improve the purity of 2D perovskite films [43].

For the two-step solution-processed method, Seok et al. exchanged DMSO molecules located in PbI_2 with FAI, because their sizes are similar while affinities are different. Besides, FAI molecules experienced ionic reaction, while DMSO reaction was Van der Waals interactions. Finally, they obtained a pure $FAPbI_3$ film without residual PbI_2 and reached a highest efficiency of 20.2%, as shown in Fig. 1(b) [44]. Zhang et al. reported that PbI_2(DMSO) intermediate not only suppresses larger grains growth, but also promotes porous PbI_2 formation during anti-solvent (Chlorobenzene) extraction (beneficial to formation intermediate), then the best device showed a superb PCE of 15.66% [45].

Apart from organic-inorganic hybrid perovskite one, inorganic and lead-free perovskite fabricated with intermediates have also been studied. Hao et al. used a facile intermediate halide exchange route to fabricate high-quality inorganic $CsPbBr_3$ film. They used intermediate (CsI-$PbBr_2$-DMSO) to displace the low-solubility CsBr, and further induced a vigorous Ostwald ripening process to make grain coarsening in annealing process, as shown in Fig. 1(c) [16]. Liu et al. introduced PbI_2(DMSO) and $PbBr_2$(DMSO) as perovskite precursor solution to displace PbI_2 and $PbBr_2$, respectively. According to Zhao et al. reported [46], they proposed that PbI_2(DMSO) and $PbBr_2$(DMSO) had the ability to reduce activation energy, which decreased the formation energy from precursor to perovskite film but the exact formation value was not given. The reduced formation energy was beneficial to obtain high-quality $CsPbI_2Br$ perovskite films at low temperature (120 °C), as shown in Fig. 1(d) [39]. Furthermore, they also used Lewis base adducts PbI_2(DMSO) and $PbBr_2$(DMSO) to form pin-hole free and large crystals perovskite films. The reason is that intermediate formed film has less concentration of seed crystals, which allows more times for growth and obtained larger grains [20]. Kanatzidis et al. obtained a holeless and uniform $FASnI_3$ perovskite by introducing SnI_2·3DMSO intermediate as precursor. Because the intermediate can promote homogeneous nucleation and adjustable the perovskite film growth rate to achieve comparable recombination lifetimes. Therefore, the carrier density of corresponding device had significantly improved (one-order larger than $MAPbI_3$-based PSCs) [47].

3.2. DMF-induced intermediate

Solvent works as carrier to dissolve solute in perovskite precursor. Boiling point (BP) and solubility are critical for obtaining homogenous perovskite film. The lower BP will form an ideal reaction environment and influence the crystallization, promoting reconstitution of perovskite film. Different from DMSO, whose BP is 189 °C while the BP of DMF is 152 °C. Besides, DMF contains lone-pair electrons on oxygen, which tends to incorporate with MAI molecule and intercalate into the PbI_2 interlayer [26]. Introducing DMF in crystalline process will form DMF-induced intermediate which showed a positive function in inhibiting uncontrolled perovskite precipitation and forming high quality perovskite film during nucleation process.

Zou et al. conducted an experiment by comparing DMF with dimethylacetamide (DMAc), and they found that DMF-induced intermediate has positive influence on high quality perovskite film [48]. This was the first time to reveal the structure of DMF-induced intermediate, as shown in Fig. 2(a). In order to make the mechanism clearer, Yang et al. conducted an extended study in 2016. They adopted a vapor induced intermediate strategy to expose perovskite film in different saturated solvent vapor atmospheres. The intermediate can induce reconstructed process, and reorganize film, leading to the perovskite film with large grain and a reduced density of trap states, as shown in Fig. 2(b) [49].

Besides, the viscosity of DMF is lower than DMSO, which greatly relates to light harvesting ability and charges separation [50]. Meng et al. used DMF as an additive during the two-step spin-coating process and found that DMF could form an amorphous phase, PbX_2-AI-DMSO-DMF (where A = FA or MA), because this amorphous phase could help MAI/FAI penetrate into the PbI_2 framework to eliminate residual precursor, and then transform it to perovskite film completely, as shown in Fig. 2(c) [28]. Though much effort has been made in DMF-induce intermediate, their structures remained a mystery. Tarasov et al. conducted a study to find the link between $CH_3NH_3PbI_3$ morphology and precursor stoichiometry in the DMF solvent. They pointed that three different intermediates ($(MA)_2(DMF)_2Pb_3I_8$, $(MA)_2(DMF)_2Pb_2I_6$ and $(MA)_3(DMF)PbI_5$) appeared when the PbI_2/MAI ratio was changing. Their structures were comprehensively investigated through Density Functional Theory (DFT) and synchrotron X-ray, as shown in Fig. 2(d) [51].

3.3. Other solvent-induced intermediates

Generally, the stability of solvent induced intermediates greatly related to their coordination ability with PbI_2. In addition to aforementioned solvents, GBL, NMP and other solvents are also used to form intermediates. All of them show different polarity, viscosity, vapour pressure and coordination with PbI_2, which leads to different morphologies and quality of perovskite films. For example, the different solvent components can control the time of processing window because of difference rate of solvent evaporation, for DMSO:DMF (9:8, v:v) reached >2 min, while for NMP:DMF (9:8, v:v) reached ~8 min [52].

Different properties of solvent can significantly influence perovskite crystal growth, and further effect the light harvesting ability and carrier separation in perovskite [50]. The detailed information of solvents and their induced intermediates are shown in Fig. 2(e). Wei et al. used micron-droplet methods to analyze the mechanism of polar aprotic solvents in perovskite crystalline process. They drew the conclusion that when the growing temperature was low, perovskite showed a needle-like intermediate, while radial domain perovskite was formed at high temperature [53]. Kim et al. extended this research by using PbI_2(DMSO) and PbI_2(NMP) as the precursor for intramolecular exchange, to form a dense, uniform and pinhole-free perovskite film. Because PbI_2(-NMP)-based perovskite film showed larger grain and longer carrier life than PbI_2(DMSO), a higher PCE of 19.5% was finally obtained [54]. Recently, Chen et al. utilized a series of green antisolvents, such as the ethers diethyl ether, anisole, diisopropyl ether (DIE), and dibutyl ether, and found that the polarity of solvent significantly influenced the purity of intermediate. Finally, using DIE as green antisolvent achieved a champion PCE of 21.26% in triple-cation FA-based PSCs [55].

Though all the related researches mentioned above showed a positive effect of solvent formed intermediates, there still existed some negative effects. Liu et al. investigated the crystallization mechanism of Ruddlesden-Popper perovskite (RDP) and pointed that superior quality, high phase purity and excellent crystal orientation can be obtained by transforming a disordered precursor solvate to perovskite phase quickly and directly without generation of intermediate. The reason is that PbI_2 crystals and solvate compound tend to form an intermediate, which will slow down inter-

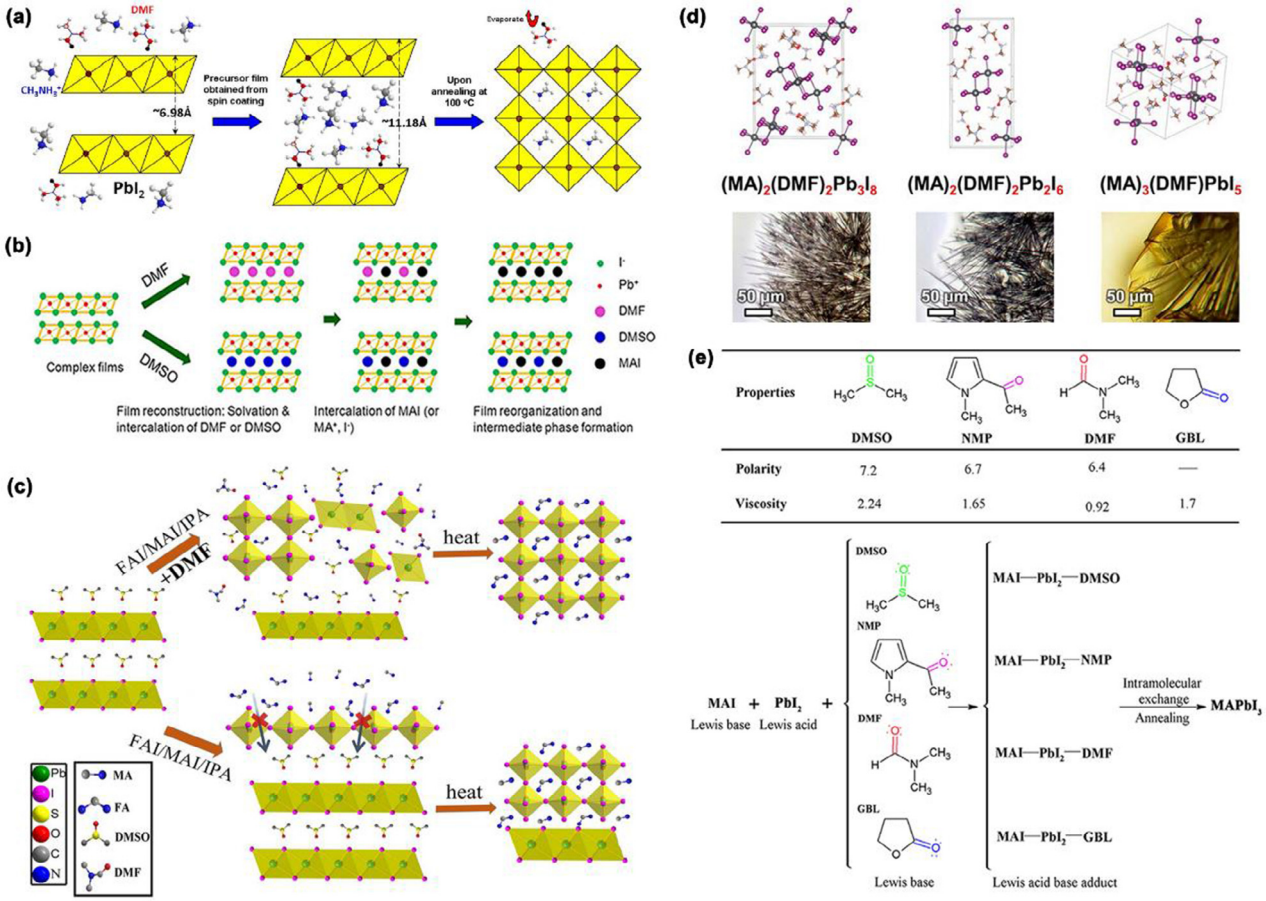

Fig. 2. (a) Schematics of the formation process of DMF-induced intermediate. Reproduced with permission [48]. Copyright 2014, The Royal Society of Chemistry publications. (b) Schematic of vapor induced intermediate strategy and its morphology evolution mechanism. Reproduced with permission [49]. Copyright 2016, American Chemical Society Publications. (c) Schematic of the reaction mechanism of DMF induced intermediates. Reproduced with permission [28]. Copyright 2017, American Chemical Society Publications. (d) Crystal structure and crystal shapes of three DMF induced intermediates. Reproduced with permission [51]. Copyright 2017, American Chemical Society Publications. (e) The molecular structure, polarity and viscosity data of DMSO, DMF, GBL and NMP and the formation processes of intermediate. Reproduced with permission [50]. Copyright 2016, Elsevier Inc Publications.

calated rate of ions and increase nucleation barrier, finally, contributing to multiple RDP phases and random orientation [18].

4. $DMAPbI_3$ ($HPbI_3$) intermediate

Zhao et al. firstly added HI and PbI_2 into DMF solvent and used the intermediate ($HPbI_3$) to fabricate $FAPbI_3$ perovskite film. Compared with other precursors formation perovskite (FA/PbI_2 with 5% HI, PCE = 10.9% and FAI/PbI_2, PCE = 4.6%), the superior property film ($FAI/HPbI_3$, PCE = 15.4%) was obtained because $HPbI_3$ can not only slow down the crystalline process by ionic exchange in the $[PbI_6]^{4-}$ octahedral framework, but also eliminate the influence of water (mainly present in HI acid) in the precursor, as shown in Fig. 3(a) [56].

Later, such intermediate was widely used in fabricating high performance inorganic PSCs [57–59], especially in the $CsPbI_3$ PSCs for conquering its instable phase problem (which spontaneously transform to instable phases at RT) [60–62]. Later, $HPbI_3$ intermediate was found to assist crystal, which is useful for obtaining high quality perovskite film with less trap states and stabilized crystal structure [63–65]. For example, Liu et al. introduced $HPbI_{3+x}$ as an intermediate additive for modifying the bandgap and increasing the stability of lattice, as shown in Fig. 3(b) [66]. Chen et al. used $HPbI_3$ to displace PbI_2 for increasing the humidity resistance of devices. They found that $HPbI_3$ intermediate served as a template for guiding the nucleation and growing of perovskite grains to induce lattice strain. The existence of tensile lattice strain can influence the phase diagram and transition temperature, as well as broaden light absorption range for making perovskite much stable, as shown in Fig. 3(c) [67]. Whereafter, Choi et al. believed that the fabricated intermediate should be H_2PbI_4, which can increase the solubility of Mn^{2+} and help Mn^{2+} dope into target lattice [68].

Nevertheless, the $HPbI_3$ synthesis process contains DMF, which will hydrolyze and generate DMA^+ ionic in solution. This question was first raised by Kanatzidis et al., who conducted a series of experiments and used amounts of apparatus to prove that $HPbI_3$-based PSCs was hybrid organic-inorganic perovskites [69]. Then Liu et al. also used $DMAPbI_3$ as additive to fabricate $Cs_xDMA_{1-x}PbI_3$ perovskite films. That $Cs_xDMA_{1-x}PbI_3$ (tolerance factor: 0.904) showed more suitable tolerance factor (t) than $CsPbI_3$ (tolerance factor: 0.851) [69,70], which will increase its structure stability because of the ideal t value (in the range of 0.9–1) [71]. In this circumstances, they obtained the best device with a PCE of 14.3% as well as better endurance, as shown in Fig. 3(d) [72].

Most recently, Zhao et al. used lots of apparatus to prove that no organic ionic existed in the lattice of $CsPbI_3$, which meant that $DMAPbI_3$-induced perovskite was inorganic perovskites [73]. In our recent work, we synthesized DMAI and $DMAPbI_x$ intermediate compounds and found that the most of DMA^+ ion was lost during the annealing process while few DMA^+ remained to dope into the

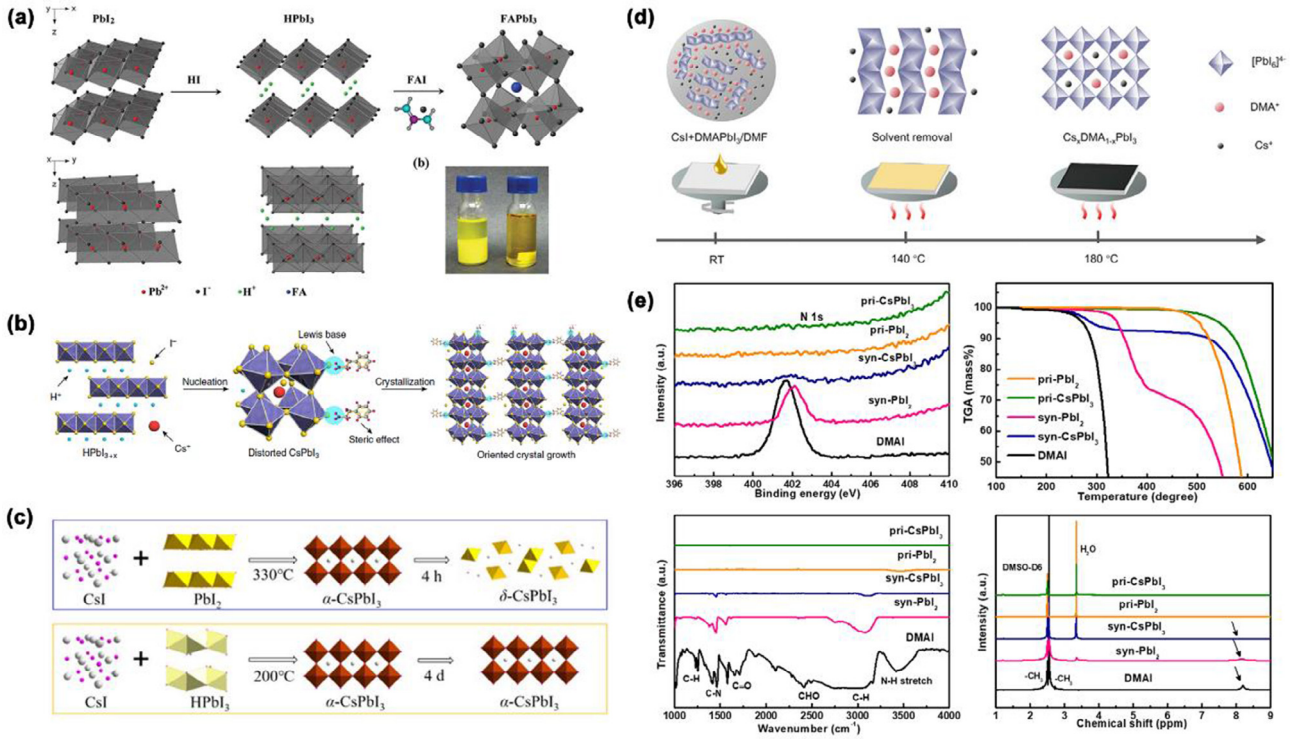

Fig. 3. (a) Schematic illustration of the configurations of PbI_2, $HPbI_3$ and $FAPbI_3$. Reproduced with permission [56]. Copyright 2015, Wiley-VCH Publications. (b) Schematic for HI/PEAI additive-induced $CsPbI_3$ crystal growth. Reproduced with permission [66]. Copyright 2018, Nature Publishing Group. (c) Schematic illustration of the $CsPbI_3$ films prepared from PbI_2- and $HPbI_3$-based precursor solutions. Reproduced with permission [67]. Copyright 2018, American Chemical Society Publications. (d) Schematic diagram of preparing $Cs_xDMA_{1-x}PbI_3$ perovskite films. Reproduced with permission [72]. Copyright 2019, Elsevier Inc Publications. (e) XPS, TGA, IR and NMR spectra for different materials. Reproduced with permission [74]. Copyright 2019, Wiley-VCH Publications.

$CsPbI_3$ crystal structure. Besides, Lewis acid-base formed at the interface when excessive DMA^+ ion reacted with Pb^{2+} to further passivate $CsPbI_3$ films and improved the device performance, as shown in Fig. 3(e) [74,75].

5. CH_3NH_2-induced intermediate

CH_3NH_2 (MA) can induce MA-based intermediate, which plays a role as defect-healing for obtaining smooth, textured, large scale and high-quality perovskite films [76]. As reported, PbI_2 has a 2D structure, which possesses strong in-plane chemical bonds and weak Van der Waals inter-plane interaction. Hence, the basic N atom with a lone pair electron in MA molecule interacts with the $[PbI_6]^{4-}$ octahedra in the layered PbI_2 structure, which can form intermediate to recrystallize the perovskite with less defect, pinhole-free and uniform.

Cui et al. developed a novel process for recrystallizing perovskite films. They pointed that MA gas can induce defect-healing by forming $CH_3NH_3PbI_3{\cdot}xCH_3NH_2$ intermediate, which could transform the rough, poor morphology perovskite into high quality films, and making corresponding device with a decent PCE of 15.1%, as shown in Fig. 4(a) [77]. Furthermore, Pan et al. studied the influence of MA gas for its inducing defect-healing property. They used MA gas to induce phase transition from rough, uneven NH_4PbI_3 non-perovskite phase to ultrasmooth, homogenate $CH_3NH_3PbI_3$ ($MAPbI_3$) perovskite directly. Because MA gas induced an intermediate to recrystallize perovskite film with low trap state, no pinhole and high-quality. From the DFT analysis, the key factors for the process of directly converting NH_4PbI_3 to $MAPbI_3$ were simultaneous presence of proton and volatile A-site alkyl group [78]. Differently, Qi et al. dissolved MA gas in ethanol to accurately control its reaction with perovskite precursor films during the annealing process. They discovered that MA gas can effectively decrease impurities at the grain boundaries and separate each grain [79].

Boyen et al. conducted a rigorous experiment to reveal the mechanism of MA gas induced defect healing with/without MA gas post-treating. They pointed that MA gas can significantly increase the infiltration rate of electron from perovskite to TiO_2 and further improve its electron injection to reduce shunting. This is proved by time-resolved photoluminescence (TRPL) measurements, the lifetime (τ_2) of carriers was greatly decreased from 10.8 ns to 8 ns after MA treatment on the top of TiO_2 [80]. The relevant experiment was also carried out by Ji et al. They found that the band gap became slightly larger after MA gas post-treating, which was beneficial to energy level aligning and carrier transporting [81]. Han et al. introduced MA gas to post-treating and photodegraded perovskite films, and then, the properties of perovskite films were much strengthened, which implied that MA gas can be used to recover pinhole and ununiform perovskite films without reconstructing or replacing any components [82]. In addition, Qi et al. introduced a simple method, exposing PbI_2 in MA gas atmosphere for forming stoichiometric $MAPbI_3$ perovskite films. The novel strategy was used in large scale because it is simple, quick and effective, as shown in Fig. 4(b) [83]. Meanwhile, MA gas induced perovskite doesn't rely on solvent or vacuum, so Han et al. used it for large scale perovskite fabrication. The MAI and PbX_2 were exposed in MA atmosphere for forming amine complex precursors, respectively. Finally, best PCE was 12.1% with an aperture area of 36.1 cm^2 square centimeters [84].

Though MA gas can induce an intermediate to heal the defect, there remain some problems. Zhou et al. proposed that MA gas has a nature of electron-donating, which can chemically reduce the poly(3,4-ethylenedioxythiophene):poly(styrenesulfonate)

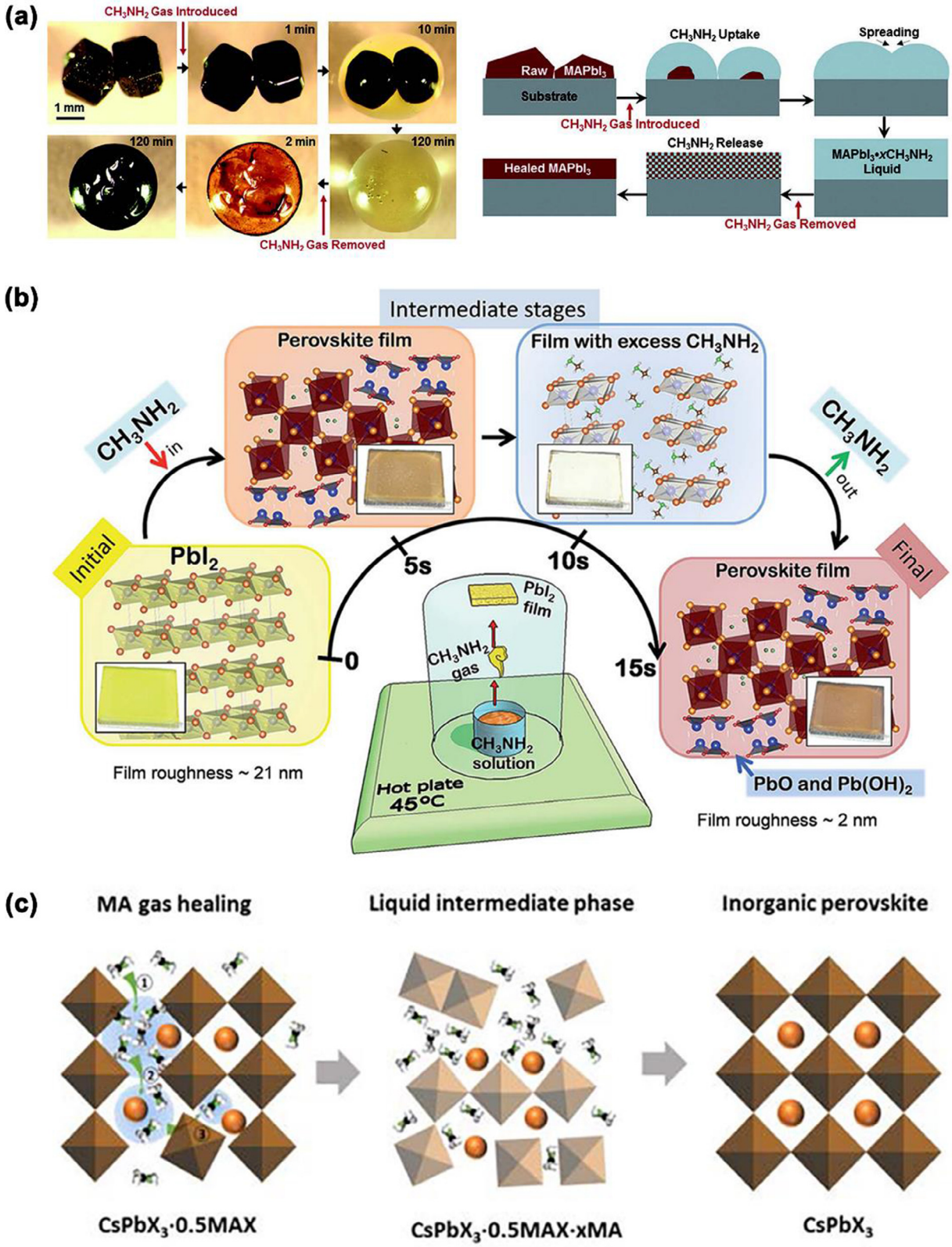

Fig. 4. (a) In situ optical images and schematic of the morphology evolution of two touching $MAPbI_3$ perovskite crystals with/without exposing to CH_3NH_2 gas. Reproduced with permission [77]. Copyright 2015, Wiley-VCH Publications. (b) The schematic of CH_3NH_2 gas induced perovskite formation. Reproduced with permission [83]. Copyright 2016, American Chemical Society Publications. (c) Schematic illustration of the CH_3NH_2 gas healing process of inorganic perovskite film with MAX additive. Reproduced with permission [86]. Copyright 2019, Wiley-VCH Publications.

(PEDOT:PSS) hole-transporting layer (HTL). The MA-reduced PEDOT:PSS showed poor conductivity and low work function, which damaged the optoelectronic properties of perovskite with PEDOT:PSS as HTL material [85].

All the aforementioned of MA-induced intermediates are hybrid organic-inorganic PSCs, which tends to form intermediate through breaking the H-bond, while H-bond is absence in inorganic perovskites. Therefore, Pang et al. used MA gas to heal $CsPbI_3$ perovskite films and introduced MA^+ for inhaling large amounts of MA gas and quickly forming a flowable liquid intermediate to heal inorganic solar cells, as shown in Fig. 4(c) [86].

6. Ionic liquid-induced intermediate

Typical solvents, such as DMSO, DMF, GBL and NMP, meet many problems. For example, DMF, GBL and NMP have high toxicity which is harmful to human body, and DMSO is a flammable solvent. In recent years, superbly efficient PSCs have to use high boiling, polar solvents, and aprotic solvents. Luckily, methylammonium acetate (MAAc) meets these criteria with nonhazardous, high viscosity and negligible vapor pressure properties.

Huang et al. used MAAc to retard the quick reaction between MAI and PbI_2 and obtained high quality perovskite films by ionic exchanger between I^- and Ac^-. Because of tremendous efforts, they achieved a high PCE of 18.09%, as shown in Fig. 5(a) [87]. Notably, from the proton nuclear magnetic resonance (^{1}H NMR) and Fourier transform infrared spectroscopy (FTIR) analysis, the final perovskite has a small amount of MAAc residue, and the residual one has high viscosity, which showed little variation with humidity and avoided moisture from destroying perovskite. Finally, the fabricated perovskite showed more humidity-resistance without obvious changes under the humidity of 80% for more than 5 months [88]. Also, the MAAc can modify morphology, so many researchers used it as additive to avoid application with anti-solvent. Tian et al. coordinated the ratio of MACl and MAAc for obtaining large grains, smooth surface and high crystallinity perovskite films, as shown in Fig. 5(b) [89].

Though MAAc can modulate the crystalline dynamics, another problem is that this process introduce excess MAAc, which can make perovskite more roughness for its high viscosity. Instead, Huang et al. used a mixture of polar aprotic DMSO and ion liquid solvent MAAc to gain large grain (nearly 9 μm) perovskite film, which showed low trap states, high carrier mobility and superb optical property, as shown in Fig. 5(c) [90].

7. Other intermediates

In addition to the aforementioned intermediates, there remain some other intermediates, which are used to control crystalline dynastic, perovskite film morphology, charge migration and so on.

In early reports, the cohesion of S-donors was stronger than O-donors [91]. Cao et al. introduced a delicate method that introduce thiourea into the perovskite precursor to control its morphology and quality for obtaining defect-free, compact and great absorption perovskite films. They pointed that thiourea can form an intermediate ($MAI{\cdot}PbI_2{\cdot}SC(NH_2)_2$) by reaction with MAI and PbI_2, which can promote grain growth and reduce its roughness during the $MAPbI_3$ perovskite formation process. And the schematic is shown in Fig. 6(a), where EA is used to extract the residual thiourea to promote crystal [92]. Moreover, 2-Aminoethanethiol (2-AET) has thiolate group, which also shows superb affinity with Pb^{2+}, and can avoid $[PbI_6]^{4-}$ octahedron tilting [93,94]. Tian et al. uniquely developed a method by introducing 2-AET as a ligand to form (PbI_2)-2-AET-(MAI) intermediate, which can retard the quick growth of PbI_2 and achieve a synchronous growth environment with MAI, as shown in Fig. 6(b) [95].

Interestingly, some ordinary solution can also induce intermediate appearing. Xu et al. introduced hydration water to induce $MAPbI_3{\cdot}xH_2O$ intermediate and manipulate its morphology, which avoided using toxic and volatile anti-solvents. After the hydration water was ingeniously introduced into the crystalline process, both the crystalline dynastic and the morphology were significantly improved, as shown in Fig. 6(c) [96]. MACl is a volatile additive and shows similar characters as DMAI [97]. Tian et al. introduced MACl to induce $MAPbI_3{\cdot}MACl$ intermediate for decelerating crystal growth. Because the intermediate can slow the release rate of PbI_2 from the $MAPbI_3{\cdot}MACl$ intermediate to control the delivery speed of PbI_2, the rapid nucleation and near thermodynamic equilibrium subsequent growth were further postponed, as shown in Fig. 6(d) [98].

Zhao et al. used an intermediate which contained crystalline solvate compound and 2D GA_2PbI_4 perovskite, to act as a scaffold for the growth of a novel 2D perovskite [99]. Fang et al. used a crystalline engineering to introduce C_{60} pyrrolidine tris-acid (CPTA) to react with PbI_2 and form CPTA:PbI_2 intermediate, which can not only reduce the nucleation by chelation of PbI_2 with the carboxylic acids of CPTA, but also increase the nucleation sites. Because the nucleation sites were largely concentrated on the surface of CPTA, and then the well-dispersed nuclei were confined in a limited space during the perovskite film growth, which led to a uneven, flat perovskite film with small domain sizes, as shown in Fig. 6(e) [22].

8. Challenges and outlook

Intermediates induced method is an effective and easy way to achieve high efficiency of PSCs. Although lots of progressive works have been done by using intermediates, there are still remained some urgent problems or unclear mechanisms. Therefore, at the end of this article, we give brief prospects for conquering these problems and further improving its performance:

8.1. Challenges

8.1.1. Unveil the mechanism of intermediate

Deep understanding the mechanism of intermediates can help researchers to improve the device's performance more efficiently. As we summarized in Table 1, the function of intermediates is diversity and without a unified statement. Most of them are based on the previous reported, but it is not suitable for perovskite with different kinds. For example, in organic-inorganic perovskite ($MAPbI_3$), PbI_2(DMSO) intermediate suppresses large grains growth and promotes porous PbI_2 formation [45], while it can decrease the activation energy from precursor to perovskite and reduce the reaction time in inorganic perovskite ($CsPbI_2Br$) [39]. Besides, the mechanism of MAAc, DMSO-induced intermediate, DMF-induced intermediate also need further exploration.

8.1.2. Inhibit side effect of intermediate

Though intermediate does a positive effect in improving device performance (eg. optimized morphology, modify energy band and improve carrier properties.) There are still remained some negative effects. As reported by Zhang et al. [18] and Mao et al. [43], intermediates showed a negative effect in fabricating 2D Ruddlesden-Popper perovskite because they slowed down intercalation of ions and increased nucleation barrier. This led to impurity appear in the produces, for which we should pay more attention to avoid intermediates appearing. Therefore, we should thoroughly investigate whether intermediates play a negative role and deliberately avoid them.

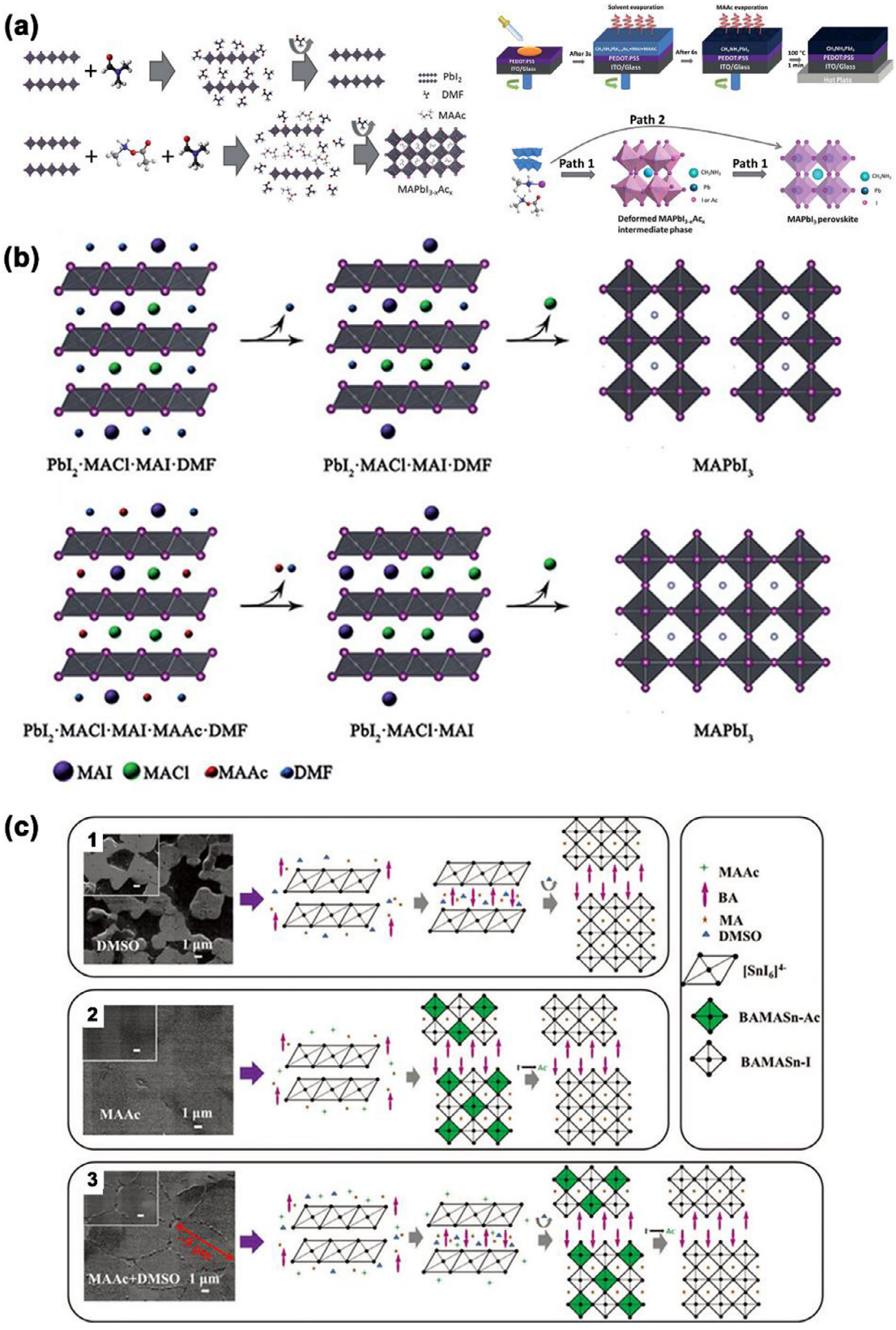

Fig. 5. (a) Three different schematic diagrams of PbI_2, MAAc, and DMF interactions. Reproduced with permission [87]. Copyright 2017, American Chemical Society Publications. (b) Schematic illustration of the formation of perovskite films from precursors with the MACl additive and the mixed additive of MACl + MAAc. Reproduced with permission [89]. Copyright 2018, American Chemical Society Publications. (c) SEM images and schematic diagrams of crystallization process of $BA_2MA_3Sn_4I_{13}$ perovskite films fabricated from different solvents (the insets are SEM images of (1) DMSO, (2) MAAc, and (3) MAAc + DMSO. The scale bars are 1 μm). Reproduced with permission [90]. Copyright 2019, Wiley-VCH Publications.

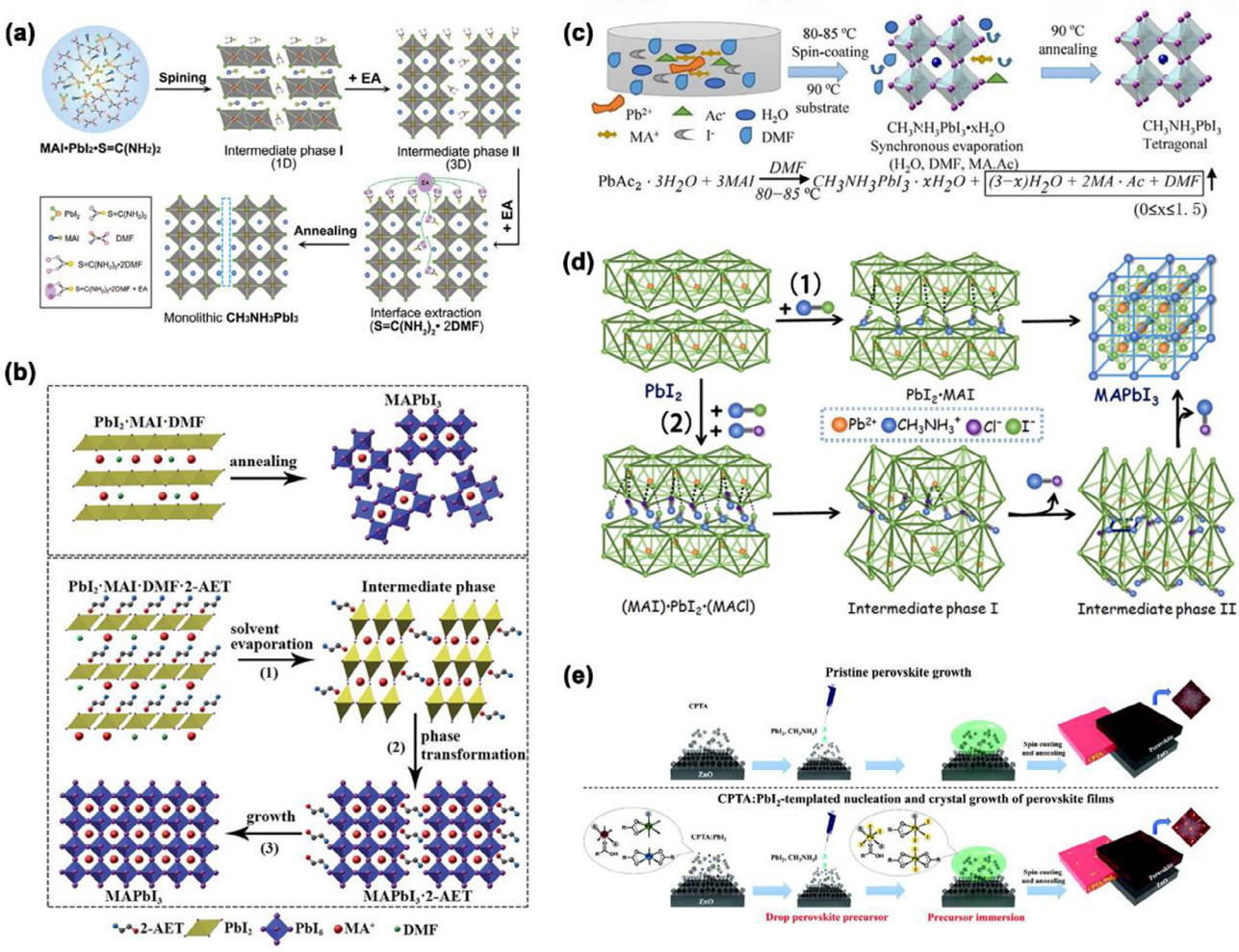

Fig. 6. (a) Schematic reaction process from the precursor to monolithic perovskite grains. Reproduced with permission [92]. Copyright 2017, Wiley-VCH Publications. (b) Schematic illustration of crystallographic conversion with/without the 2-AET additive during the annealing process. Reproduced with permission [95]. Copyright 2016, American Chemical Society Publications. (c) Illustration of thin film growth mechanism for the $PbAc_2$-based perovskite via hydration water induced intermediate together with HASP method. Reproduced with permission [96]. Copyright 2018, American Chemical Society Publications. (d) The reaction process in the different perovskite fabrication routes: (1) Normal anti-solvent precipitation method, (2) MACl introduced anti-solvent precipitation method. Intermediate I represent the complex of $MAPbI_3$, $MAPbI_2Cl$, $(CH_3NH_3)_{x+y}PbI_{2+x}Cl_y$ and PbI_2, while intermediate II represent the lattice distorted $MAPbI_3$ and the residual MACl. Reproduced with permission [98]. Copyright 2016, Elsevier Inc Publications. (e) Proposed mechanism of perovskite crystal formation on the CPTA thin films without and with PbI_2 nuclei; the assisted formation of the $[PbI_6]^{4-}$ octahedra in the CPTA:PbI_2 adducts is also illustrated. Reproduced with permission [22]. Copyright 2018, Wiley-VCH Publications.

8.1.3. Stabilize the intermediate components

The interaction of intermediate usually is Van der Waals, which is week and will be easily destroyed. What's more, some intermediates (eg. DMSO-induced intermediate, $MAPbI_{3-x}Ac_x$ intermediate) will decompose into harmful by-produce and damage perovskite morphology [37,100]. Therefore, it's an urgent problem need to solve for improving PSCs performance before their commercial application.

8.2. Future directions

8.2.1. Assistant with equipment to illustrate the mechanism

The mechanism analysis can assist with some advanced equipments (eg. grazing incident wide-angle X-ray (GIWAX), in-suit X-ray diffraction (XRD), transmission electron microscopy (TEM)) or theoretical modeling to deal with them. Especially, from a microcosmic perspective to monitor the crystal kinetics change or element distribution during the growth of perovskite film, and unveil the detail mechanism of intermediate.

8.2.2. Develop intermediate for low temperature fabrication

$CsPbI_3$ meets an unstable phase problem (black perovskite phase will transform to non-perovskite phase), while metastable phase can be obtained under low temperature for improving its stability [59]. Luckily, as mentioned above, Grätzel et al. used intermediate to fabrication perovskite films and obtained the best PCE of 18.1% without annealing process, and it could satisfy with $CsPbI_3$ perovskite [23]. Meanwhile, this simple and useful strategy shows greatly potential applications in wearable, soft electronic devices.

8.2.3. Adopt intermediate in large area perovskite film fabrication

As we discussed above, MA gas can induce defect-healing and widely applied in three-dimension (3D) perovskite to obtain pinhole-free, uniform and compact perovskite. This method shows rapid reaction process and lower demand of precursor film quality, which attracts in large scale commercial production [101]. Therefore, a broad development prospects remained in commercial application.

8.2.4. Use intermediate in low dimension perovskite system

Reducing dimension can induce quantum confinement effect, surface effect and structural effect to increase the perovskite stability. For example, Liu et al. used PEAI to fabricated 2D $(PEA)_2(Cs)_{n-1}$-$PbnI_{3n+1}$ and increase its stability [2]. The optimized device kept 88% of initial values while 3D γ-$CsPbI_3$ PSCs degraded to ~69% when heating 80 °C in nitrogen atmosphere. However, the corresponding works are lack and great effort should be took.

8.2.5. Boost performance of other perovskites via intermediate

Nearly all the intermediates mentioned above are related to $MAPbI_3$ and inorganic $CsPbX_3$ PSCs. There is a dearth of effort in other types PSCs. For example, the FA-based perovskite possessed a broader light-harvesting spectrum and the collection of longer-wave-length photons, which shows superior performances, compared with $MAPbI_3$-based perovskite [102]. Therefore, a broad development prospects is also remained in this filed.

Declaration of Competing Interest

The authors declare that they have no known competing financial interests or personal relationships that could have appeared to influence the work reported in this paper.

Acknowledgments

This work was funded by the National Natural Science Foundation of China (51902148, 61704099, 51801088 and 11664001), the Fundamental Research Funds for the Central Universities (lzujbky-2020-61, lzujbky-2019-88 and lzujbky-2020-kb06), and the Special Funding for Open and Shared Large-Scale Instruments and Equipments of Lanzhou University (LZU-GXJJ-2019C023 and LZU--GXJJ-2019C019).

References

[1] H. Wang, H. Bian, Z. Jin, H. Zhang, L. Liang, J. Wen, Q. Wang, L. Ding, S.F. Liu, Chem. Mater. 31 (2019) 6231–6238.
[2] K. Wang, Z. Li, F. Zhou, H. Wang, H. Bian, H. Zhang, Q. Wang, Z. Jin, L. Ding, S. Liu, Adv. Energy Mater. 9 (2019) 1902529.
[3] W. Hu, H. Cong, W. Huang, Y. Huang, L. Chen, A. Pan, C. Xue, Light: Sci. Appl. 8 (2019) 106.
[4] L. Gu, Z. Fan, Light: Sci. Appl. 6 (2017) e17090.
[5] NREL, NREL, 2019, https://www.nrel.gov/pv/device-performance.html.
[6] F. Zhou, Z. Li, H. Chen, Q. Wang, L. Ding, Z. Jin, Nano Energy 73 (2020) 104757.
[7] Y. Gao, Y. Dong, K. Huang, C. Zhang, B. Liu, S. Wang, J. Shi, H. Xie, H. Huang, S. Xiao, J. He, Y. Gao, R.A. Hatton, J. Yang, ACS Photon. 5 (2018) 4104–4110.
[8] G. Liu, C. Zhou, F. Wan, K. Li, Y. Yuan, Y. Gao, Y. Lu, B. Yang, Appl. Phys. Lett. 113 (2018) 3501.
[9] C. Liu, K. Wang, C. Yi, X. Shi, A.W. Smith, X. Gong, A.J. Heeger, Adv. Funct. Mater. 26 (2016) 101–110.
[10] W.-J. Yin, J.-H. Yang, J. Kang, Y. Yan, S.-H. Wei, J. Mater. Chem. A 3 (2015) 8926–8942.
[11] Y.-C. Zhao, W.-K. Zhou, X. Zhou, K.-H. Liu, D.-P. Yu, Q. Zhao, Light: Sci. Appl. 6 (2017) e16243.
[12] A.J. Ramadan, L.A. Rochford, S. Fearn, H.J. Snaith, J. Phys. Chem. Lett. 8 (2017) 4172–4176.
[13] H.-H. Fang, F. Wang, S. Adjokatse, N. Zhao, J. Even, M. Antonietta Loi, Light: Sci. Appl. 5 (2016) e16056.
[14] D. Xin, Z. Wang, M. Zhang, X. Zheng, Y. Qin, J. Zhu, W.-H. Zhang, ACS Sustain. Chem. Eng. 7 (2019) 4343–4350.
[15] Y. Zhou, O.S. Game, S. Pang, N.P. Padture, J. Phys. Chem. Lett. 6 (2015) 4827–4839.
[16] W. Zhu, M. Deng, Z. Zhang, D. Chen, H. Xi, J. Chang, J. Zhang, C. Zhang, Y. Hao, ACS Appl. Mater. Interfaces 11 (2019) 22543–22549.
[17] P. Shi, Y. Ding, Y. Ren, X. Shi, Z. Arain, C. Liu, X. Liu, M. Cai, G. Cao, M.K. Nazeeruddin, S. Dai, Adv. Sci. 5 (2019) 1901591.
[18] X. Zhang, R. Munir, Z. Xu, Y. Liu, H. Tsai, W. Nie, J. Li, T. Niu, D.-M. Smilgies, M. G. Kanatzidis, A.D. Mohite, K. Zhao, A. Amassian, S.F. Liu, Adv. Mater. 30 (2018) 1707166.
[19] J. Jiang, Q. Wang, Z. Jin, X. Zhang, J. Lei, H. Bin, Z.-G. Zhang, Y. Li, S. Liu, Adv. Energy Mater. 8 (2018) 1701757.
[20] G. Yin, H. Zhao, H. Jiang, S. Yuan, T. Niu, K. Zhao, Z. Liu, S.F. Liu, Adv. Funct. Mater. 28 (2018) 1803269.
[21] Z. Li, F. Zhou, Q. Wang, L. Ding, Z. Jin, Nano Energy 71 (2020) 104634.
[22] Y.-C. Wang, J. Chang, L. Zhu, X. Li, C. Song, J. Fang, Adv. Funct. Mater. 28 (2018) 1706317.
[23] T. Matsui, J.-Y. Seo, M. Saliba, S.M. Zakeeruddin, M. Grätzel, Adv. Mater. 29 (2017) 1606258.
[24] A. Marronnier, G. Roma, S. Boyer-Richard, L. Pedesseau, J.-M. Jancu, Y. Bonnassieux, C. Katan, C.C. Stoumpos, M.G. Kanatzidis, J. Even, ACS Nano 12 (2018) 3477–3486.
[25] C.-H. Kang, I. Dursun, G. Liu, L. Sinatra, X. Sun, M. Kong, J. Pan, P. Maity, E.-N. Ooi, T.K. Ng, O.F. Mohammed, O.M. Bakr, B.S. Ooi, Light: Sci. Appl. 8 (2019) 94.
[26] J.-W. Lee, H.-S. Kim, N.-G. Park, Acc. Chem. Res. 49 (2016) 311–319.
[27] D. Huang, T. Goh, J. Kong, Y. Zheng, S. Zhao, Z. Xu, A.D. Taylor, Nanoscale 9 (2017) 4236–4243.
[28] J. Wu, X. Xu, Y. Zhao, J. Shi, Y. Xu, Y. Luo, D. Li, H. Wu, Q. Meng, ACS Appl. Mater. Interfaces 9 (2017) 26937–26947.
[29] N. Li, C. Shi, M. Lu, L. Li, G. Xiao, Y. Wang, Superlattices Microstruct. 100 (2016) 179–184.
[30] Y. Liu, Y. Zhang, Z. Yang, H. Ye, J. Feng, Z. Xu, X. Zhang, R. Munir, J. Liu, P. Zuo, Q. Li, M. Hu, L. Meng, K. Wang, D.-M. Smilgies, G. Zhao, H. Xu, Z. Yang, A. Amassian, J. Li, K. Zhao, S.F. Liu, Nat. Commun. 9 (2018) 5302.
[31] A.G. Ortoll-Bloch, H.C. Herbol, B.A. Sorenson, M. Poloczek, L.A. Estroff, P. Clancy, Cryst. Growth Des. 20 (2020) 1162–1171.
[32] C.C. Coleman, H. Goldwhite, W. Tikkanen, Chem. Mater. 10 (1998) 2794–2800.
[33] Y. Wu, A. Islam, X. Yang, C. Qin, J. Liu, K. Zhang, W. Peng, L. Han, Energy Environ. Sci. 7 (2014) 2934–2938.
[34] J. Cao, X. Jing, J. Yan, C. Hu, R. Chen, J. Yin, J. Li, N. Zheng, J. Am. Chem. Soc. 138 (2016) 9919–9926.
[35] X. Fu, N. Dong, G. Lian, S. Lv, T. Zhao, Q. Wang, D. Cui, C.-P. Wong, Nano Lett. 18 (2018) 1213–1220.
[36] P. Wang, X. Zhang, Y. Zhou, Q. Jiang, Q. Ye, Z. Chu, X. Li, X. Yang, Z. Yin, J. You, Nat. Commun. 9 (2018) 2225.
[37] N. Ahn, D.-Y. Son, I.-H. Jang, S.M. Kang, M. Choi, N.-G. Park, J. Am. Chem. Soc. 137 (2015) 8696–8699.
[38] H. Zhang, J. Cheng, D. Li, F. Lin, J. Mao, C. Liang, A.K.-Y. Jen, M. Gratzel, W.C.H. Choy, Adv. Mater. 29 (2017) 1604695.
[39] H. Jiang, J. Feng, H. Zhao, G. Li, G. Yin, Y. Han, F. Yan, Z. Liu, S. Liu, Adv. Sci. 5 (2018) 1801117.
[40] N.J. Jeon, J.H. Noh, Y.C. Kim, W.S. Yang, S. Ryu, S.I. Seok, Nat. Mater. 13 (2014) 897–903.
[41] M. Yin, F. Xie, H. Chen, X. Yang, F. Ye, E. Bi, Y. Wu, M. Cai, L. Han, J. Mater. Chem. A 4 (2016) 8548–8553.
[42] M. Jahandar, J.H. Heo, C.E. Song, K.-J. Kong, W.S. Shin, J.-C. Lee, S.H. Im, S.-J. Moon, Nano Energy 27 (2016) 330–339.
[43] P. Mao, J. Zhuang, Y. Wei, N. Chen, Y. Luan, J. Wang, Solar RRL 3 (2019) 1800357.
[44] W.S. Yang, J.H. Noh, N.J. Jeon, Y.C. Kim, S. Ryu, J. Seo, S.I. Seok, Science 348 (2015) 1234–1237.
[45] J. Zhang, G. Zhai, W. Gao, C. Zhang, Z. Shao, F. Mei, J. Zhang, Y. Yang, X. Liu, B. Xu, J. Mater. Chem. A 5 (2017) 4190–4198.
[46] Y. Wang, T. Zhang, F. Xu, Y. Li, Y. Zhao, Solar RRL 2 (2018) 1700180.
[47] F. Hao, C.C. Stoumpos, P. Guo, N. Zhou, T.J. Marks, R.P.H. Chang, M.G. Kanatzidis, J. Am. Chem. Soc. 137 (2015) 11445–11452.
[48] D. Shen, X. Yu, X. Cai, M. Peng, Y. Ma, X. Su, L. Xiao, D. Zou, J. Mater. Chem. A 2 (2014) 20454–20461.
[49] L. Zuo, S. Dong, N.D. Marco, Y.-T. Hsieh, S.-H. Bae, P. Sun, Y. Yang, J. Am. Chem. Soc. 138 (2016) 15710–15716.
[50] J. Chen, Y. Xiong, Y. Rong, A. Mei, Y. Sheng, P. Jiang, Y. Hu, X. Li, H. Han, Nano Energy 27 (2016) 130–137.
[51] A.A. Petrov, I.P. Sokolova, N.A. Belich, G.S. Peters, P.V. Dorovatovskii, Y.V. Zubavichus, V.N. Khrustalev, A.V. Petrov, M. Grätzel, E.A. Goodilin, A.B. Tarasov, J. Phys. Chem. C. 121 (2017) 20739–20743.
[52] M. Yang, Z. Li, M.O. Reese, O.G. Reid, D.H. Kim, S. Siol, T.R. Klein, Y. Yan, J.J. Berry, M.F.A.M. van Hest, K. Zhu, Nat. Energy 2 (2017) 17038.
[53] Y. Li, L. Zhi, G. Ge, Z. Zhao, X. Cao, F. Chen, X. Cui, F. Lin, L. Ci, J. Sun, D. Zhuang, J. Wei, Cryst. Growth Des. 19 (2018) 959–965.
[54] Y. Jo, K.S. Oh, M. Kim, K.-H. Kim, H. Lee, C.-W. Lee, D.S. Kim, Adv. Mater. Interfaces 3 (2016) 1500768.
[55] L. Wang, X. Wang, L.-L. Deng, S. Leng, X. Guo, C.-H. Tan, W.C.H. Choy, C.-C. Chen, Mater. Horiz. 7 (2019) 934–942.
[56] F. Wang, H. Yu, H. Xu, N. Zhao, Adv. Funct. Mater. 25 (2015) 1120–1126.
[57] Y. Fu, M.T. Rea, J. Chen, D.J. Morrow, M.P. Hautzinger, Y. Zhao, D. Pan, L.H. Manger, J.C. Wright, R.H. Goldsmith, S. Jin, Chem. Mater. 29 (2017) 8385–8394.
[58] H. Bian, D. Bai, Z. Jin, K. Wang, L. Liang, H. Wang, J. Zhang, Q. Wang, S. Liu, Joule 2 (2018) 1500–1510.
[59] J.A. Steele, H. Jin, I. Dovgaliuk, R.F. Berger, T. Braeckevelt, H. Yuan, C. Martin, E. Solano, K. Lejaeghere, S.M.J. Rogge, C. Notebaert, W. Vandezande, K.P.F. Janssen, B. Goderis, E. Debroye, Y.-K. Wang, Y. Dong, D. Ma, M. Saidaminov, H. Tan, Z. Lu, V. Dyadkin, D. Chernyshov, V.V. Speybroeck, E.H. Sargent, J. Hofkens, M.B.J. Roeffaers, Science 365 (2019) 679–684.
[60] J. Zhang, D. Bai, Z. Jin, H. Bian, K. Wang, J. Sun, Q. Wang, S. Liu, Adv. Energy Mater. 8 (2018) 1703246.
[61] L. Liang, M. Liu, Z. Jin, Q. Wang, H. Wang, H. Bian, F. Shi, S. Liu, Nano Lett. 19 (2019) 1796–1804.
[62] Q. Wang, Z. Jin, D. Chen, D. Bai, H. Bian, J. Sun, G. Zhu, G. Wang, S. Liu, Adv. Energy Mater. 8 (2018) 1800007.

[63] T. Zhang, M.I. Dar, G. Li, F. Xu, N. Guo, M. Grätzel, Y. Zhao, Sci. Adv. 3 (2019) e1700841.
[64] J.-F. Liao, H.-S. Rao, B.-X. Chen, D.-B. Kuang, C.-Y. Su, J. Mater. Chem. A 5 (2017) 2066–2072.
[65] Y. Jiang, J. Yuan, Y. Ni, J. Yang, Y. Wang, T. Jiu, M. Yuan, J. Chen, Joule 2 (2018) 1356–1368.
[66] K. Wang, Z. Jin, L. Liang, H. Bian, D. Bai, H. Wang, J. Zhang, Q. Wang, S. Liu, Nat. Commun. 9 (2018) 4544.
[67] S. Xiang, Z. Fu, W. Li, Y. Wei, J. Liu, H. Liu, L. Zhu, R. Zhang, H. Chen, ACS Energy Lett. 3 (2018) 1824–1831.
[68] J. Xi, C. Piao, J. Byeon, J. Yoon, Z. Wu, M. Choi, Adv. Energy Mater. 9 (2019) 1901787.
[69] W. Ke, I. Spanopoulos, C.C. Stoumpos, M.G. Kanatzidis, Nat. Commun. 9 (2018) 4785.
[70] J. Zhang, G. Hodes, Z. Jin, S. Liu, Angew. Chem. Int. Ed. 58 (2019) 15596–15618.
[71] A. Dutta, N. Pradhan, ACS Energy Lett. 4 (2019) 709–719.
[72] Y. Pei, Y. Liu, F. Li, S. Bai, X. Jian, M. Liu, iScience 15 (2019) 165–172.
[73] Y. Wang, M.I. Dar, L.K. Ono, T. Zhang, M. Kan, Y. Li, L.j. Zhang, X. Wang, Y. Yang, X. Gao, Y. Qi, M. Grätzel, Y. Zhao, Science 365 (2019) 591–595.
[74] H. Bian, H. Wang, Z. Li, F. Zhou, Y. Xu, H. Zhang, Q. Wang, L. Ding, S.F. Liu, Z. Jin, Adv. Sci. 7 (2020) 1902868, https://doi.org/10.1002/advs.201902868.
[75] Z. Li, Z. Jin, J. Semicond. (2020), https://doi.org/10.1088/1674-4926/41/5/051202.
[76] T. Zhao, S.T. Williams, C.-C. Chueh, D.W. deQuilettes, P.-W. Liang, D.S. Ginger, A.K.Y. Jen, RSC Adv. 6 (2016) 27475–27484.
[77] Z. Zhou, Z. Wang, Y. Zhou, S. Pang, D. Wang, H. Xu, Z. Liu, N.P. Padture, G. Cui, Angew. Chem. Int. Ed. 54 (2015) 9705–9709.
[78] Y. Zong, Y. Zhou, M. Ju, H.F. Garces, A.R. Krause, F. Ji, G. Cui, X.C. Zeng, N.P. Padture, S. Pang, Angew. Chem. Int. Ed. 55 (2016) 14723–14727.
[79] Y. Jiang, E.J. Juarez-Perez, Q. Ge, S. Wang, M.R. Leyden, L.K. Ono, S.R. Raga, J. Hu, Y. Qi, Mater. Horiz. 3 (2016) 548–555.
[80] B. Conings, S.A. Bretschneider, A. Babayigit, N. Gauquelin, I. Cardinaletti, J. Manca, J. Verbeeck, H.J. Snaith, H.-G. Boyen, ACS Appl. Mater. Interfaces 9 (2017) 8092–8099.
[81] M.-J. Zhang, N. Wang, S.-P. Pang, Q. Lv, C.-S. Huang, Z.-M. Zhou, F.-X. Ji, A.C.S. Appl, Mater. Interfaces 8 (2016) 31413–31418.
[82] L. Hong, Y. Hu, A. Mei, Y. Sheng, P. Jiang, C. Tian, Y. Rong, H. Han, Adv. Funct. Mater. 27 (2017) 1703060.
[83] S.R. Raga, L.K. Ono, Y. Qi, J. Mater. Chem. A 4 (2016) 2494–2500.
[84] H. Chen, F. Ye, W. Tang, J. He, M. Yin, Y. Wang, F. Xie, E. Bi, X. Yang, M. Grätzel, L. Han, Nature 550 (2017) 92–95.
[85] T. Liu, F. Jiang, J. Tong, F. Qin, W. Meng, Y. Jiang, Z. Li, Y. Zhou, J. Mater. Chem. A 4 (2016) 4305–4311.
[86] Z. Shao, Z. Wang, Z. Li, Y. Fan, H. Meng, R. Liu, Y. Wang, A. Hagfeldt, G. Cui, S. Pang, Angew. Chem. Int. Ed. 58 (2019) 5587–5591.
[87] Y. Xia, C. Ran, Y. Chen, Q. Li, N. Jiang, C. Li, Y. Pan, T. Li, J. Wang, W. Huang, J. Mater. Chem. A 5 (2017) 3193–3202.
[88] L. Chao, Y. Xia, B. Li, G. Xing, Y. Chen, W. Huang, Chem 5 (2019) 995–1006.
[89] M. Wang, B. Li, P. Siffalovic, L.-C. Chen, G. Cao, J. Tian, J. Mater. Chem. A 6 (2018) 15386–15394.
[90] J. Qiu, Y. Xia, Y. Chen, W. Huang, Adv. Sci. 6 (2019) 1800793.
[91] I. Wharf, T. Gramstad, R. Makhija, M. Onyszchuk, Can. J. Chem. 54 (1976) 3430–3438.
[92] C. Fei, B. Li, R. Zhang, H. Fu, J. Tian, G. Cao, Adv. Energy Mater. 7 (2017) 1602017.
[93] H. Fleischer, D. Schollmeyer, Inorg. Chem. 43 (2004) 5529–5536.
[94] N.C. Li, R.A. Manning, J. Am. Chem. Soc. 77 (1955) 5225–5228.
[95] B. Li, C. Fei, K. Zheng, X. Qu, T. Pullerits, G. Cao, J. Tian, J. Mater. Chem. A 4 (2016) 17018–17024.
[96] X. Zhou, Y. Zhang, W. Kong, M. Hu, L. Zhang, C. Liu, X. Li, C. Pan, G. Yu, C. Cheng, B. Xu, J. Mater. Chem. A 6 (2018) 3012–3021.
[97] Y. Wang, X. Liu, T. Zhang, X. Wang, M. Kan, J. Shi, Y. Zhao, Angew. Chem. Int. Ed. 58 (2019) 16691–16696.
[98] C. Fei, L. Guo, B. Li, R. Zhang, H. Fu, J. Tian, G. Cao, Nano Energy 27 (2016) 17–26.
[99] Y. Zhang, P. Wang, M.-C. Tang, D. Barrit, W. Ke, J. Liu, T. Luo, Y. Liu, T. Niu, D.-M. Smilgies, Z. Yang, Z. Liu, S. Jin, M.G. Kanatzidis, A. Amassian, S.F. Liu, K. Zhao, J. Am. Chem. Soc. 141 (2019) 2684–2694.
[100] Y. Guo, X. Yin, J. Liu, W. Chen, S. Wen, M. Que, H. Xie, Y. Yang, W. Que, B. Gao, Org. Electron. 65 (2019) 207–214.
[101] C. Li, S. Pang, H. Xu, G. Cui, Sol. RRL 1 (2017) 1700076.
[102] J. Liu, Y. Shirai, X. Yang, Y. Yue, W. Chen, Y. Wu, A. Islam, L. Han, Adv. Mater. 27 (2015) 4918–4923.